Dalton Transactions

Ruthenium(II) Complexes of N-Heterocyclic Carbenes Derived from Imidazolium-linked Cyclophanes.

Journal:	*Dalton Transactions*
Manuscript ID:	DT-ART-05-2014-001473.R1
Article Type:	Paper
Date Submitted by the Author:	21-Jul-2014
Complete List of Authors:	Caramori, Giovanni; Universidade Federal de Santa Catarina, Departamento de Química Garcia, Leone; Universidade Federal de Santa Catarina, Departamento de Química Andrada, Diego; Philipps-Universität Marburg, Fachbereich Chemie Frenking, G; Philipps-Universität Marburg, Fachbereich Chemie

SCHOLARONE™
Manuscripts

CREATED USING THE RSC LaTeX PCCP ARTICLE TEMPLATE – SEE www.rsc.org/electronicfiles FOR DETAILS

ARTICLE TYPE www. rsc.org/xxxxxx | XXXXXXXX

Ruthenium(II) Complexes of N-Heterocyclic Carbenes Derived from Imidazolium-linked Cyclophanes.†

Giovanni F. Caramori,*[a,b] Leone C. Garcia,[a] Diego M. Andrada,[b] and Gernot Frenking[b]

Received Xth XXXXXXXXXX 20XX, Accepted Xth XXXXXXXXX 20XX

First published on the web Xth XXXXXXXXXX 200X

DOI: 10.1039/b000000x

The present work seeks to characterize, in the light of electronic structure calculations, the unusual metal-[(η^1-NHC)$_2$: (η^6-arene)] bonding situation in a set of ruthenium(II) complexes containing the *ortho*-xylylene-linked-bis(NHC)cyclophane ligand (NHC-cyclophane) (**1**), which binds to ruthenium center through two carbene carbons and one of the arene rings. The nature of ruthenium(II)-[(η^1-NHC)$_2$: (η^6-arene)] bonding was investigated in the light of EDA-NOCV, NBO and QTAIM analyses by adopting **1** as model compound. The interplay between the *ortho*-cyclophane scaffold in different families of five-membered carbenes such as imidazole **1**, triazole-based NHCs (Enders' carbenes), **2**, and P-heterocyclic carbenes, PHCs, **3**, was investigated. The metal-[(η^1-NHC)$_2$: (η^6-arene)] bonding situation was also extended to the heavier analogues such N-heterocyclic silylenes (NHSi) and N-heterocyclic germylenes (NHGe), in order to address how the basicity of NHC, NHSi and NHGe is affected by the cyclophane framework. The results reveal that the ruthenium(II)-[(η^1-NHC)$_2$: (η^6-arene)] are more covalently than electrostatically bonded and the degree of covalence is larger in PHCs than in NHCs or Enders' carbenes. They also reveal that the covalent character in ruthenium(II)-[(η^1-NHGe)$_2$: (η^6-arene)] and ruthenium(II)-[(η^1-NHSi)$_2$: (η^6-arene)] bonds is larger than in ruthenium(II)-[(η^1-NHC)$_2$: (η^6-arene)].

1 Introduction

Cyclophanes are defined as compounds containing two or more aromatic rings held by saturated or unsaturated chains as alternate components of a large ring (Figure 1).[1] The cyclophane chemistry has emerged as central field in chemistry,[2–7] connecting different areas,[5] such as organic, organometallic, physical chemistry, supramolecular chemistry, catalysis, polymer chemistry, conducting materials, and others.[8–19] Cyclophanes present unusual structural features especially due to the electronic interactions between the aromatic rings.[20–24] The most important characteristic of cyclophanes, as revealed particularly from photoelectron and ESR studies,[25,26] is the interaction of the two aromatic decks to give one overall π-electron system. This π-electron delocalization over the whole molecular structure is also observed in multilayered [2_n]cyclophanes.[27]

Cyclophanes have attracted the interest of chemists for a long time, specially due to their structural versatility and ability to form transition metal complexes through non-covalent cation-π interactions.[25,26] A large number of cyclophane-metal complexes including different kinds of metals such as Cr, Mo, W, Fe, Ru, Os, Co, Rh, Ir, Ni, Cu, Ag, and others is known.[7,28–30] The discovery of Creutz-Taube[31] compound has spurred a large amount of work about electron transfer properties of mixed-valence ions in bimetallic complexes. In this scenario, Virgil Boekelheide[2,32–38] provided an outstanding contribution to the cyclophane chemistry, specially regarding the systhesis of mixed valence ruthenophanes and their structural and electronic properties.

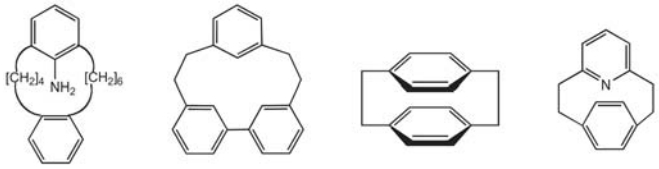

Fig. 1 Examples of cyclophanes; (a) 2,2-Amino[6.4]*ortho* -metacyclophane, (b) [2.2.0]metacyclophane, (c) [2.2]paracyclophane, (d) [2]paracyclo-[2](2,6)pyridinophane.

Azolium-linked cyclophanes are compounds in which two aromatic moieties are connected by two or more azolium units. They are considered a sub-set of the cyclophane family, in which azolium groups are part of the macrocyclic structure (Figure 2).[39–43] Azolium-linked cyclophanes have attracted the attention in the scientific community for differ-

† Electronic Supplementary Information (ESI) available: [details of any supplementary information available should be included here]. See DOI: 10.1039/b000000x/

[a] *Departamento de Química, Universidade Federal de Santa Catarina, CP 476, Florianópolis, SC, 88040-900, Brazil. Fax: +55 48 3721-6852; Tel: +55 48 3721-6839; E-mail: giovanni.caramori@ufsc.br*

[b] *Fachbereich Chemie - Philipps-Universität Marburg, Hans-Meerwein-Strasse, D-35032, Marburg, Germany*

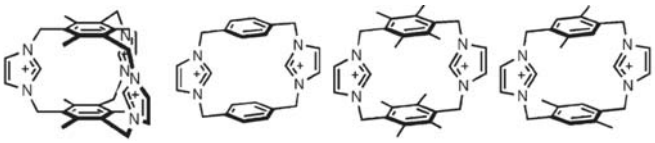

Fig. 2 Examples of azolium-linked *para*-cyclophanes

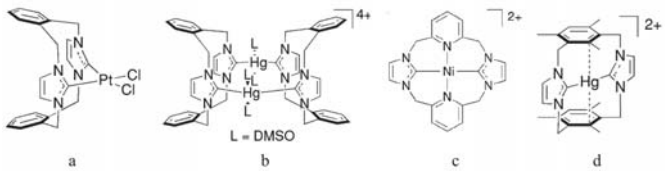

Fig. 3 Examples of coordination modes of NHC-cyclophanes

ent reasons, including synthetic challenges, host-guest chemistry in anion recognition,[44–46] conformational dynamics,[42] and the outstanding potential to act as precursors of NHCs (N-heterocyclic carbenes) metal complexes.[47–55] The deprotonation of the corresponding azolium-linked cyclophane salts by the use of suitable bases provides the corresponding N-heterocyclic carbenes. NHC-cyclophane ligands can display a large range of coordination modes, for instance (i) involving only carbene carbons of the NHC components of the macrocycle (Figure 3a), (ii) leading to the formation of dinuclear complexes (Figure 3b), (iii) presenting binding modes that involve heteroatoms or donor groups belonging the cyclophane structure (Figure 3c), (iv) or still presenting metal-arene interactions, which are dependent on the cyclophane conformer (Figure 3d). The properties of complexes containing NHC-cyclophane ligands are many-sided, including catalytic behaviour, luminescent properties, and potential antitumor behaviour.[47–56]

Recently, Baker and coworkers[56] synthesized a ruthenium(II) complex containing an *ortho*-xylylene-linked-bis(NHC)cyclophane ligand (NHC-cyclophane) (**1**), with a very peculiar coordination mode, in which the two NHCs and the arene that constitute the *ortho*-cyclophane macrocyclic structure bind to the metal center simultaneously, (Figure 4). According to Baker and coworkers,[56] the Ru(II) ion in **1** is four-coordinated to the chlorine atom, to the pair of carbene donors, and to one of the bridging aromatic rings, in a coordination mode like [(η^1-NHC)$_2$: (η^6-arene)], for which only few examples have been reported.[57–60] Complexes based on **1** can be employed to investigate the interplay between the extended π-system of cyclophanes and the σ-donating ability of carbenes, by varying both the cyclophane scaffold and the sort of heterocyclic carbene employed, for instance NHCs, PHCs, CAACs, cyclopropenylidene, Enders' carbenes,[61] and others.

In this paper, the effects of different NHC-cyclophane macrocyclic structures on the nature of the metal-[(η^1-NHC)$_2$: (η^6-arene)] bonding are evaluated, by adopting Baker's complex, **1**, (Figure 4) as prototype, by keeping the same *ortho*-cyclophane structure and by changing the family of five-membered carbene such as imidazole (NHCs) **1**, triazole-based NHCs (Enders' carbenes), **2**, and P-heterocyclic carbenes (PHCs), **3**.[62–67] The presence of π-donating heteroatoms (N or P) attached directly to the carbenic carbon yields a stable singlet ground state and decreases the electron deficiency of the carbene center. However, the π-donor capability of heteroatoms depends on the planar configurations that they can exhibit.[62–68] For instance, the phosphorus π-donation capability can be larger than the nitrogen if planarity around the phosphorus atom can be achieved.[62–68] Similarly, such investigation is extended to the isostructural analogues of NHC, N-heterocyclic silylenes, NHSi,[69–74] (**4**-**6**) and N-heterocyclic germylenes, NHGe,[75–80] (**7**-**9**) in order to stand the differences in the metal-ligand bonding between the carbene complexes **1**-**3**, silylene **4**-**6** and germylene **7**-**9** homologues, by addressing the stabilization of the metal-ligand bonds of NHC, NHSi and NHGe in the cyclophane framework (Figure 4). In the present paper, the metal-ligand bonding of complexes **1**-**9** is investigated in the light of the EDA-NOCV, QTAIM and NBO analyses.

2 Computational Methods

The geometries of complexes **1**-**9** (Figures 4 and 5) were optimized without constraints at the non-local DFT level of theory,[81,82] with the exchange functional of Becke[83] and the correlation functional of Perdew[84] in conjunction with the atom pairwise dispersion correction, BP86-D3,[85–87] and the Ahlrichs triple-ζ-quality basis set, def2-TZVP,[88,89] The BP86-D3/def2-TZVP model was employed with scalar relativistic effects, the zero-order regular approximation, ZORA.[90–92] All geometry optimizations were performed employing the ORCA package.[93] The model BP86-D3/def2-TZVP used for geometry optimization has provided data in excellent agreement with available X-ray structure data of **1**,[56] as shown in the supporting information (Table S1 and Figure S1). All reported structures, **1**-**9**, were characterized as minimum on the potential energy surfaces by the absence of imaginary eigenvalues in the Hessian matrix. The nature of the interactions between [RuCl]$^+$ and the ligands, was investigated using the EDA-NOCV approach.[94] The charge distribution in the complexes was calculated with NBO partition scheme.[95–98] The bonding situation in the complexes was also analyzed by means of the quantum theory of atoms in molecules, QTAIM.[99,100]

The EDA-NOCV[94] calculations were also performed using BP86-D3/TZ2P+ model,[101] in conjunction with the zero-order regular approximation, ZORA, as implemented in

 This journal is © The Royal Society of Chemistry [year]

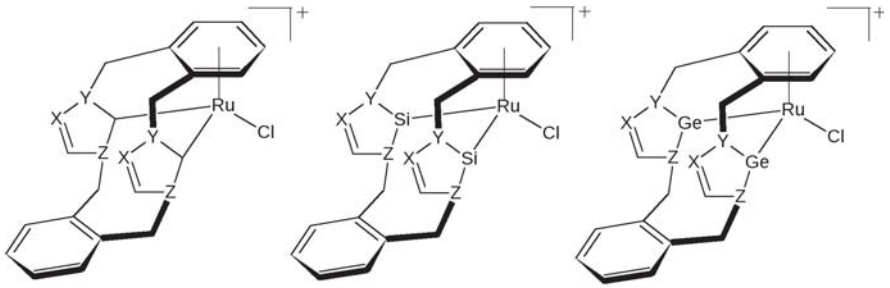

1 x = CH; y = z = N
2 x = y = z = N
3 x = N, y = z = P
4 x = CH; y = z = N
5 x = y = z = N
6 x = N, y = z = P
7 x = CH; y = z = N
8 x = y = z = N
9 x = N, y = z = P

Fig. 4 Schematic representation of ortho-cyclophane-NHC complex (**1**), and ruthenium(II) model complexes containing *ortho*- cyclophane with Enders' carbenes (**2**) and PHCs (**3**). Silylenes (**4**-**6**) and germylenes (**7**-**9**) homologues are also represented.

ADF2013 software.[102,103] The EDA-NOCV approach is a combination of extended transition state method, ETS,[104,105] with the natural orbitals for chemical valence scheme, NOCV.[106–109] The ETS scheme decomposes the interaction energy, ΔE^{int}, into different components, (1). ΔE^{ele} corresponds to the classical electrostatic interactions between the interacting fragments, ΔE^{Pauli} accounts for the repulsive Pauli interaction between the occupied orbitals of the fragments, and ΔE^{orb} describes both the interactions between occupied molecular orbitals of one fragment with the unoccupied orbitals of the other fragments and the inner-fragment polarization. The NOCV pairs (ψ_{-i}, ψ_i) decomposes the differential density, $\Delta\rho(r)$, into contributions $\Delta\rho_i(r)$, (2), where ν_i and N stands for the NOCV eigenvalues and the number of basis functions, respectively. The deformation density, $\Delta\rho_i(r)$, provides information about symmetry and the direction of the flow of charge. In the EDA-NOCV scheme, the orbital component, ΔE^{orb}, is stated in terms of the eigenvalues ν_i, (2), where $F_{i,i}^{TS}$ are the diagonal transition-state Kohn-Sham matrix elements defined over NOCV eigenvalues. The components ΔE_i^{orb} provide the energetics estimation of the $\Delta\rho_i(r)$, related with a particular electron flow channel for the bonding between two interacting fragments. Since BP86-D3 functional is employed, the dispersion correction, ΔE^{disp}, is added to the ΔE^{int} values to describe the total bond energy, (1) . Further information regarding the fundamentals and applications of EDA-NOCV can be found in the following literature.[94,106–114]

$$\Delta E^{\text{int}} = \Delta E^{\text{ele}} + \Delta E^{\text{Pauli}} + \Delta E^{\text{orb}} + \Delta E^{\text{disp}} \qquad (1)$$

$$\Delta\rho(r) = \sum_{i=1}^{N/2} \nu_i \left[-\psi_{-i}^2(r) + \psi_i^2(r)\right] = \sum_{i=1}^{N/2} \Delta\rho_i(r) \qquad (2)$$

$$\Delta E^{\text{orb}} = \sum_i \Delta E_i^{\text{orb}} = \sum_{i=1}^{N/2} \nu_i \left[-F_{-i,-i}^{TS} + F_{i,i}^{TS}\right] \qquad (3)$$

The contributions of singlet, triplet and quintet states were computed using CASSCF.[115–117] All these *ab initio* calculations were performed using MOLPRO 2012.1 program package.[118,119] Two structural motives were employed for the ligands **1** and **3**. On the one hand, the ligands as they are in the complex have been computed YHC(big) and, on the other, the small models where the EHC moieties were kept while the remaining atoms were erased YHC(small). Active space of the CASSCF method included from the positive combination of sp^2 carbene lone pairs to the negative combination of the p_z carbene orbitals.

3 Results and discussion

3.1 Geometries

All complexes, **1**-**9**, were calculated by considering (NHC)cyclophane and (PHC)cyclophane ligands in the singlet state.[78] Since NHCs have four possible electronic states,[78] and the NHC-cyclophane ligand contain two NHCs, the occurrence of a possible quintet state for this ligands was taken into account. The singlet-quintet gap was evaluated by considering the NHC-cyclophane ligand in the geometry of the complex. The singlet-quintet gap values NHC-cyclophane ligand in **1** is 130.0 kcal.mol^{-1}, while for homologues containing Si, **4**, and Ge, **7**, the values are 102.6 and 97.4 kcal.mol^{-1}, respectively (Figure S1, supporting information). The presence of triazole-based in the complexes **2**, **5**, and **8**, increases even more the singlet-quintet gap, with values 133.9, 112.6, and 118.2 kcal.mol^{-1}, for **2**, **5**, and **8**, respectively. This can be

explained in terms of the relative energies of sp^n and p type orbitals of the carbene and how their energies change in the presence of different heteroatoms.[78] CASSCF/def2-SVP calculations of ligands **1** and **3** considering an active space which includes the lone pairs sp^2 until the p_z carbene formally empty orbitals (Tables S2 and S3), predict the singlet state to be the lowest in energy for both compounds.

The geometry optimizations were performed by considering the structure of **1** as a prototypical test case for the evaluation of structural parameters, since the crystallographic data are available (Figure S2 and Table S1, supporting information). The optimized structure (BP86-D3/def2-TZVP) reproduces the crystallographic parameters of **1** very well (Figures 5, S2 and Table S1), confirming that the ruthenium atom is roughly four-coordinated by chlorine, the carbenes $(\eta^1-\text{NHC})_2$ and the centroid (Ru-X = 1.756 Å) of one of the aromatic rings, (η^6-arene) (Figure 5), as also observed by Baker.[56] The ruthenium atom is not equidistant from carbons belonging to the bridging xylylene aromatic ring. In fact, it is closer to the bridgehead carbons (2.096 Å (exp. 2.091 Å)) than to the other carbons, in which the Ru-C distances range from 2.309 Å (exp. 2.274 Å) to 2.376 Å (exp. 2.330 Å). The calculated ruthenium-carbene distances are equivalent and equal to 2.008 Å, in agreement with the crystallographic distances (2.034 and 2.038 Å). The calculated geometric parameters of **1**-**3** are presented in Figure 5 and the paremeters of **4**-**9** are presented in Figure S3 (support information).

The calculations predict the following trend for bond distances Ru-Ge > Ru-Si > Ru-C, which is observed not only in complexes with NHCs (**1**, **4**, and **7**), but also in those containing Enders' carbenes (**2**, **5**, and **8**), and PHCs (**3**, **6**, and **9**) (Figures 5 and S3). For instance, in complexes **1**, **4**, and **7**, the Ru-C, Ru-Si, and Ru-Ge bond lengths are 2.008, 2.235, and 2.459 Å, respectively. On going from complexes containing NHCs, **1**, **4**, **7**, to those with Enders' carbenes, **2**, **5**, **8**, no substantial differences are observed in the Ru-C, Ru-Si, and Ru-Ge bond distances. On the other hand, the smallest values of Ru−C, Ru−Si, and Ru−Ge bond lengths are observed when PHCs are present, **3**, **6**, and **9**. Complexes containing NHCs or Enders' carbenes, **1**-**2**, **4**-**5**, **7**-**8**, present planar coordination around the nitrogen atoms, as can be observed by the sum of the three bond angles around the nitrogen atom, $\sum\Phi_N$, which present values close or equal to 360° (Figures 5 and S3). On the other hand, structures of complexes **3**, **6**, and **9** display the five-membered heterocyclic rings with anti-pyramidalization. According to Schoeller and Eisner,[63] it is characteristic of singlet ground states. The *syn*-pyramidalization was not observed for these structures. As it has been already observed by Boehme and Frenking,[120] a remarkable characteristic of the NHCs and PHCs is the decrease of internal angles, Y-E-Z (E = C, Si, Ge), at the donor atoms of **1**-**9** and the increase of E-Y and E-Z (E = C, Si, Ge) bond distances on going from C to Ge (Figures 5 and S3), which is a consequence of the increasing atomic size of donor atoms. These findings are substantiated by the Wiberg bond indexes (Figure 6). The E-Y and E-Z (E = C, Si, Ge) bond length values are slightly different and dependend on the nature of the carbene employed (diamino, Enders's or diphosphino). For instance, in complexes containing diamino (**1**, **4**, **7**) and diphosphino carbenes (**6**, **9**) E-Y > E-Z, while in complexes containing Enders' carbenes (**2**, **5**, **8**) and diphosphino carbene **3** the opposite trend is observend, E-Y < E-Z (Figures 5 and S3).

Geometry optimizations reveal that the spacial orientation of PHC rings in **3** is opposite to the PHSi and PHGe orientation in **6** and **9** (Figures 5 and S3). The geometry optimizations of **3**-**6** were performed by mimicking the structure of **1** as starting geometry. Since the structures of **3**-**6** comprise four phosphorus atoms, different degrees of pyramidalization can be achieved, ending up different conformations. In fact, a systematic conformational search was performed by varying the degree of anti-pyramidalization of the phosphorus atoms, and two local minima were found for complexes **3**, **6**, and **9**. Figure S4 (supporting information) shows the difference of energy between these conformers. Only the most stable conformers of **3**-**9** were considered for the bonding analysis. The degree of pyramidalization of phosphorus atom, $\sum\Phi_P$, is directly related to the quintet-singlet gap of the ligands. For instance, the nitrogen atoms in **1** are in a perfectly planar environment (Figure 5), $\sum\Phi_N = 360°$, whereas the phosphorus centers in **3** present the largest *anti*-pyramidalization, $\sum\Phi_P = 326.9°$ and $\sum\Phi_P = 314.1°$. Consequently, the singlet-quintet gap drops from 130 kcal.mol^{-1} to 33.7 kcal.mol^{-1} (Figure S1). The ligands of complexes **3**, **6** and **9** present different quintet-singlet gaps, the smallest value is observed for **3** (33.7 kcal.mol^{-1}) and the largest for **6** (80.2 kcal.mol^{-1}), while **9** presents an intermediate value (54.2 kcal.mol^{-1}). The largest quintet-singlet gap observed for **6** can be explained with the presence of two phosphorus atoms in an almost perfect planar environment, $\sum\Phi_P = 358.5°$, while an intermediate value is found in **9** $\sum\Phi_P = 338.6°$. The other two phosphorus centers in **6** and **9** are considerably pyramidalized, presenting $\sum\Phi_P = 304.8°$ and $\sum\Phi_P = 291.4°$, respectively (Figure S3). The results show that the cyclophane framework has therefore a non-negligible effect on planarity of the phosphorus environment.

3.2 Bonding Analysis

Table 1 shows the EDA-NOCV results for complexes **1**-**9**, in which the interactions between the Ru(II)Cl$^+$ ion (1) and different *ortho*-xylylene-linked-*bis*(YHE)cyclophane ligands (Y = N, P; E = C, Si, Ge) (2) are evaluated. For complexes **1**-**9**, it is observed that the Ru(II)-NHC bonds are stronger than Ru(II)-NHSi and Ru(II)-NHGe. For instance, ΔE^{int} val-

 This journal is © The Royal Society of Chemistry [year]

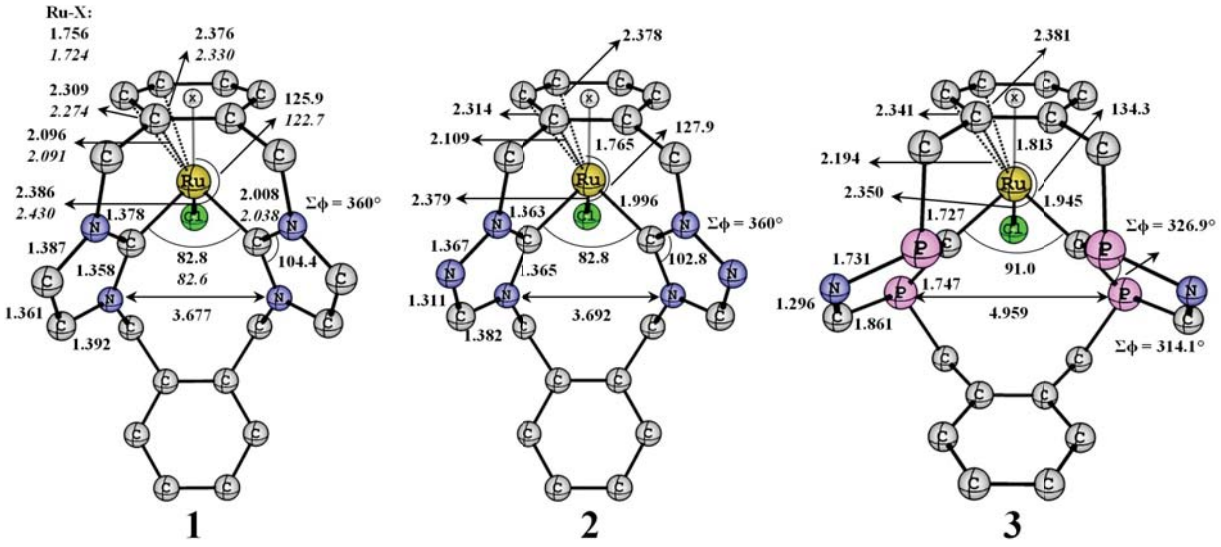

Fig. 5 Optimized structures of complexes **1**-**3**, employing BP86-D3/def2-TZVP as level of theory. Selected crystallographic parameters of **1** are presented in *italics*.

ues for complexes **1**, **4**, and **7** are -338.3, -280.9 and -250.4 kcal.mol^{-1}, respectively. The strongest bond in **1** is also manifested in the shortest ruthenium-carbene bond distance, (Figure 5), in the largest bond orders (Figure 6) and in the $\rho(r)$ value at the bcp (Figure 8). The reduction in the metal-ligand bond strength of **4**, and **7** is due to the electrostatic component, ΔE^{elstat}, which decreases significantly on going from **1** (-387.1 kcal.mol^{-1}) to **4** (-269.1 kcal.mol^{-1}) and **7** (-224.4 kcal.mol^{-1}), while the orbital contribution, ΔE^{orb}_{tot}, is almost similar in these complexes (-440.7, -439.4 and -395.4 kcal.mol^{-1}) (Table 1). These results are in full agreement with the difference of charge between the interacting fragments, q_1 and q_2, which is larger in **1** than in **4** and **7** (Table 1). The NPA atomic charges also support this trend (Figure 7a). On going from complexes containing NHCs (**1**, **4**, **7**) to complexes with triazolinylidene (Enders' carbene) (**2**, **5**, **8**), the metal-ligand bond strength is slightly decreased. For example, ΔE^{int} values for complexes **1** and **2** are -338.3 and -326.7 kcal.mol^{-1}, respectively. The metal-ligand bond strength decrease is attribbuted to both ΔE^{elstat} and ΔE^{orb}_{tot}, which diminish on going from **1** to **2**. Such trend is also observed in the heavier homologues complexes, **4**, **5**, **7** and **8**.

In comparison with complexes containing NHC, **1**, or triazolinylidene, **2**, the complex with PHC, **3**, presents the strongest metal-ligand interaction (-345.0 kcal.mol^{-1}), which is due to the increase of the orbital term ΔE^{orb}_{tot} and the decrease of the electrostatic contributions. This behaviour is also confirmed by the shortest Ru-C bond lengths (Figure S3), largest bond orders (Figure 6) and by the largest $\rho(r)$ at the bcp (Figure 8). In fact, the ratios between attractive interactions (ΔE^{elstat} / ΔE^{orb}_{tot}) show that the orbital interactions are more pronouced in PHC (**3**) than in NHC (**1** and **2**) complexes, while the electrostatic interactions are more important in NHC (**1** and **2**) complexes. These findings are also supported by the quantitative analysis of the frontier orbitals for the interacting fragments (Figures 9 and S5). By comparing the left columns in Figures 9 and S5, it is possible to observe that the HOMO-LUMO gap is much smaller in **3** than in **1**. In addition, the LUMO in **1** does not have enough symmetry to support a Ru-NHC π-back-donation, while the PHC has orbitals ready for Ru-PHC π-back-donation, with adequate symmetry and lower energy in comparison with the NHC frontier orbitals. These observations are paralleled by the change in singlet-quintet gaps when going from NHC (130.0 kcal.mol^{-1}) to PHC (33.7 kcal.mol^{-1}). These results are in agreement with the previous work of Jacobsen,[65] in which the author verified that PHCs form bonds with transition metal complexes in strength comparable or large to those of NHC, and also observes that PHCs are more likely to undergo π-back-donation when compared with NHCs.

The EDA-NOCV results indicate that in **1**-**9** the interacting fragments are more covalently than electrostatically bonded. The high covalent character of Ru(II)-ligand bond, apparently in disagreement with some previous works,[121–123] can be easily understood in terms of the bonding situation in which the metal-ligand bond involves the simultaneous interaction of a Ru(II)Cl$^+$ ion with to carbenic carbons and the aromatic ring of the cyclophane, presenting a more covalent than electrostatic character. The Ru(II)Cl$^+$-arene interaction is responsible for the increase of the covalent character, as we have re-

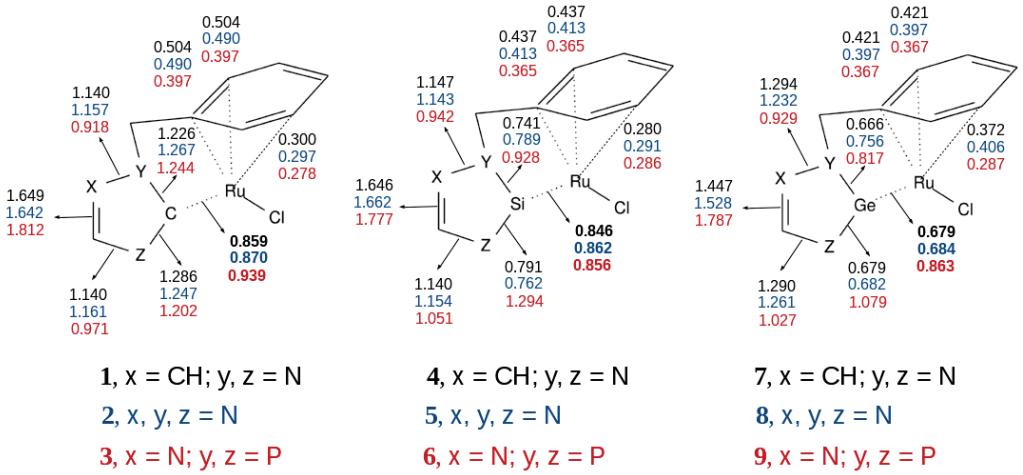

Fig. 6 Wiberg bond indices (values obtained in the NAO basis) of complexes **1**-**9**.

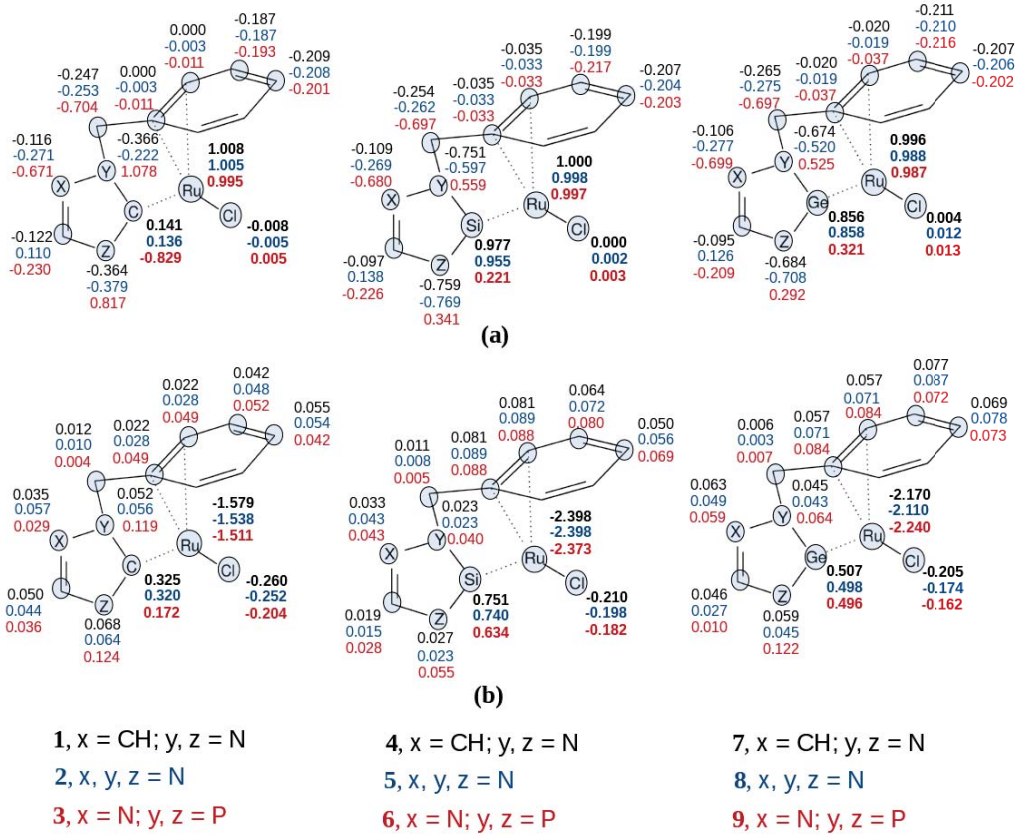

Fig. 7 Schematic representation of NPA atomic charge of the interacting fragments Ru(II)Cl^{+} (1) and η^1-(NHE)$_2$,(η^6-arene) (2), isolated **(a)** and in the complexes **1**-**9** geometries **(b)**.

This journal is © The Royal Society of Chemistry [year]

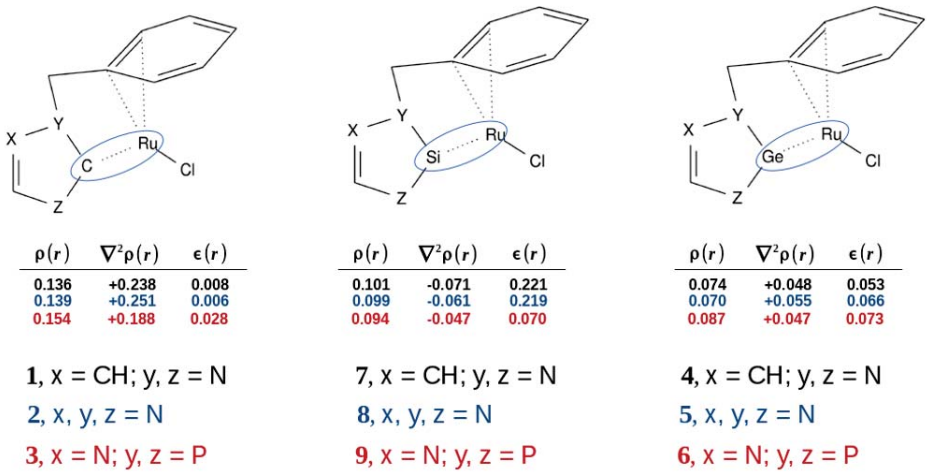

Fig. 8 Schematic representation of Ru-C, Ru-Si, and Ru-Ge bond critical points properties (a.u.) in the complexes **1**-**9**.

Table 1 EDA-NOCV of complexes **1**-**9** (kcal.mol^{-1}) at BP86-D3/TZ2P+, in which Ru(II)Cl^{+} (1) and η^1-(carbene)$_2$.(η^6-arene) (2) are the interacting fragments.

	C			Si			Ge		
	1	**2**	**3**	**4**	**5**	**6**	**7**	**8**	**9**
ΔE^{int}	-338.3	-326.7	-345.0	-280.9	-266.3	-273.1	-250.4	-231.9	-261.9
ΔE^{Pauli}	506.8	500.8	508.7	439.4	427.9	398.6	381.3	372.9	359.0
ΔE^{elstat}	-387.1	-375.8	-364.9	-269.1	-252.9	-240.8	-224.4	-211.3	-214.6
	(46.8%)[b]	(46.4%)	(43.8%)	(38.0%)	(37.0%)	(36.6%)	(36.2%)	(35.6%)	(35.3%)
ΔE^{orb}_{tot}	-440.7	-434.7	-468.0	-439.4	-430.1	-416.6	-395.4	-382.0	-393.5
	(53.2%)	(53.6%)	(56.2%)	(62.0%)	(63.0%)	(63.4%)	(63.8%)	(64.4%)	(64.7%)
ΔE^{orb}_{1}	-148.5	-147.5	-166.6	-197.4	-190.9	-184.6	-172.1	-161.2	-172.9
ΔE^{orb}_{2}	-92.7	-90.6	-88.2	-81.6	-80.8	-79.0	-77.3	-76.3	-72.7
ΔE^{orb}_{3}	-54.7	-53.5	-46.7	-35.6	-33.1	-32.6	-30.6	-30.9	-36.0
ΔE^{orb}_{4}	-27.5	-28.3	-39.6	-29.4	-30.2	-27.9	-29.4	-26.0	-27.3
ΔE^{orb}_{5}	-21.3	-21.6	-21.6	-23.4	-23.4	-20.8	-16.6	-16.3	-16.0
ΔE^{orb}_{6}	-13.0	-13.2	-16.8	-11.6	-11.5	-12.3	-14.0	-14.4	-11.8
ΔE^{orb}_{7}	-9.8	-9.5	-14.9	-9.4	-9.9	-10.2	-10.2	-10.6	-10.3
ΔE^{orb}_{8}	-9.5	-9.0	-10.9	-9.4	-9.8	-10.1	-9.9	-10.6	-9.8
ΔE^{orb}_{9}	-9.1	-8.6	-8.8	-8.7	-7.6	-6.5	-4.5	-5.1	-5.9
ΔE^{orb}_{10}	-8.9	-8.6	-7.4	-2.5	-2.3	-2.3	-3.8	-2.5	-2.7
ΔE^{orb}_{11}	-7.3	-7.0	-4.8	-2.3	-2.0	-2.3	-2.3	-2.3	-2.1
ΔE^{orb}_{res}	-38.4	-37.7	-41.7	-28.1	-28.6	-28.0	-24.7	-25.8	-26.0
ΔE^{disp}	-17.2	-17.0	-20.9	-11.7	-11.1	-14.4	-11.8	-11.5	-12.8
q^a_1	0.735	0.735	0.838	0.605	0.607	0.605	0.568	0.601	0.620
q_2	0.265	0.265	0.162	0.395	0.393	0.395	0.432	0.399	0.380

[a] (q_1) and (q_2) are the Hirshfeld charges for fragments.

[b] Values in parentheses give the percentage of attractive interactions (ΔE^{elstat} and ΔE^{orb})

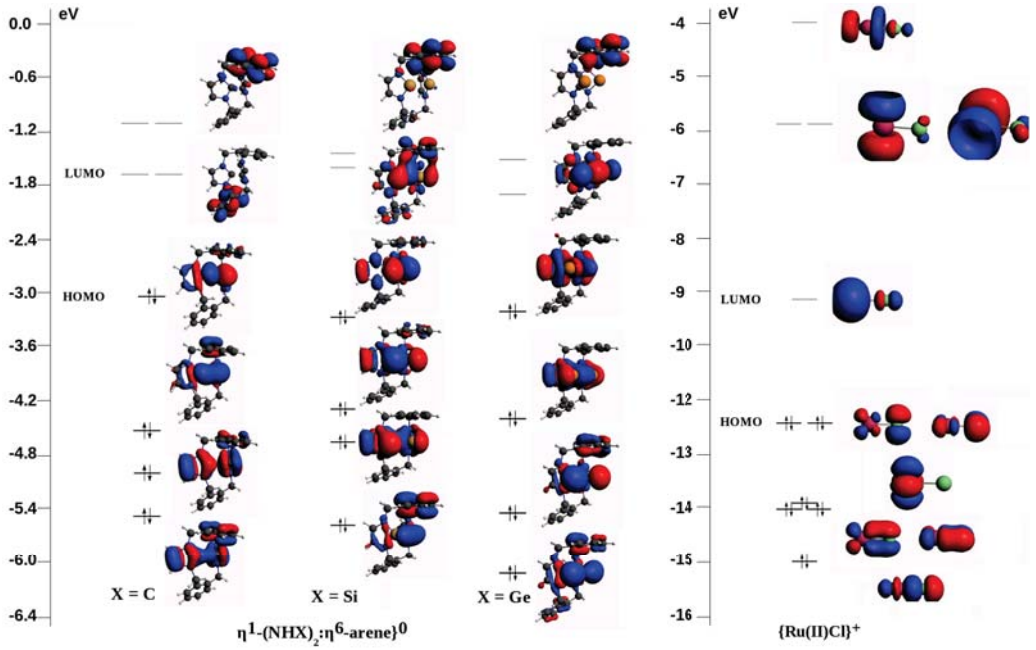

Fig. 9 Quantitative diagram of the frontier orbitals for the interacting fragments in **1**, **4**, and **7**.

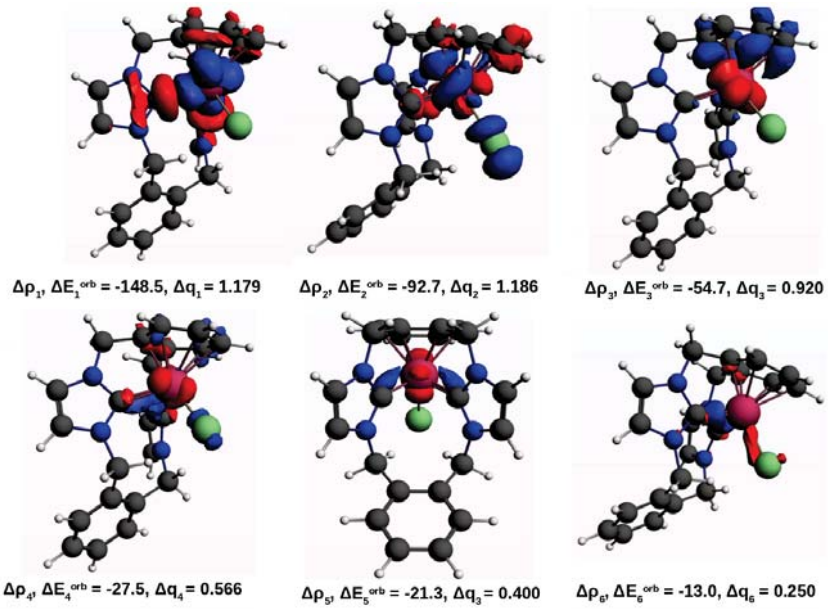

Fig. 10 Contours of deformation densities , $\Delta\rho_i(r)$, describing the interaction between Ru(II)Cl$^+$ and η^1-(NHC)$_2$.(η^6-arene) fragments in **1** and their corresponding energy , ΔE_i^{orb} (kcal.mol^{-1}), and charge estimation, $\Delta q_i = \nu_i$ (a.u.). Red and blue surfaces indicate density outflow and density inflow, respectively (contour value 0.003).

This journal is © The Royal Society of Chemistry [year]

cently reported,[124] the nature of cation-π interactions in a set of $[Ru(\eta^6-C_{16}H_{12}R_4)(NH_3)_3]^{2+}$ is more covalent the electrostatic as determined by two different energy decomposition schemes Su-Li EDA and EDA-NOCV. The results obtained by both analyses are entirely in line, showing that in ruthenium-arene interactions the covalent character is greater than the electrostatic character and that the dominant density deformations come from donation and back-donation between the interacting fragments.[124]

For complexes containing carbenes, **1**-**3**, the electrostatic term contributes 43.8 - 46.8%, and it is still smaller in the heavier analogues **4**-**9**, contributing with 35.3 - 38.0% to the attractive interactions. Therefore, the orbital contribution, ΔE_{tot}^{orb}, is much more significant in heavier analogs, silylenes (**4**-**6**) and germylenes (**7**-**9**), than in carbenes (**1**-**3**). The quantitative diagram of frontier orbitals of **1**, **4**, and **7** justifies this trend (Figure 9). In NHC and PHC complexes (**1**-**3**) the orbital contribution ranges from 53.2% to 56.2%, in silylenes (**4**-**6**) and germylenes (**7**-**9**) it ranges from 62.0% to 64.7%. Also in these cases, the largest orbital contributions are observed for PHSi and PHGe complexes (**4** and **9**) (Table 1). The increase of the orbital contribution in detriment of the electrostatic contribution results from the decrease of the charge difference between the interacting fragments in complexes containing silylenes (**4**-**6**) and germylenes (**7**-**9**), (Figure 7a). The frontier orbital diagram (Figure 9) makes clear that the heavier analogues, silylenes **4** and germylenes **7**, have the LUMO locate at the NHSi anf NHGe portions of the *ortho*-xylylene-linked-bis(NHE)cyclophane ligands, making them more favorable to the metal-ligand π-back-donation, while the LUMO and LUMO+1 of the corresponding carbene **1** belong to the aromatic moieties of the *ortho*-xylylene-linked-bis(NHE)cyclophane ligand.

According to Figure 10, in complex **1** the dominant density deformation, $\Delta\rho_1$ arises from the ligand-metal donation and comprises the donation (*red surfaces denote density outflow, blue surfaces density inflow*) from both the carbene and the aromatic ring that directly interacts with the $Ru(II)Cl^+$ fragment. The amount of charge transfered is $\Delta q_1 = 1.179$ e. Such charge transfer corresponds to the highest energetic stabilization ΔE_1^{orb} = -148.5 kcal.mol^{-1}. The second more stabilizing density deformation $\Delta\rho_2$ involves both a ligand-metal donation and a density polarization of ruthenium atom towards the chloride ion, providing ΔE_2^{orb} = -92.7 kcal.mol^{-1} as energetic stabilization. The tree following density deformations $\Delta\rho_3$, $\Delta\rho_3$, and $\Delta\rho_5$ (Table 1, Figure 10) characterize the presence of metal-ligand back-donation, which provide the following stabilization ΔE_3^{orb} = -54.7 kcal.mol^{-1}, ΔE_4^{orb} = -27.5 kcal.mol^{-1}, and ΔE_5^{orb} = -21.3 kcal.mol^{-1}, respectively. These values clearly show that in **1** the ligand-metal donation is more significant than the metal-ligand back-donation. The other less significant orbital contributions ΔE_6^{orb}, ΔE_9^{orb} and ΔE_{res}^{orb} comprise density deformation channels $\Delta\rho_6(r)$-$\Delta\rho_9(r)$ related with the different sort of density polarization in the structure of the complexes, specially due to the cyclophane framework.

According to Table 1, the energetic estimation ($\Delta E_1^{orb} - \Delta E_9^{orb}$) of deformation densities, present a very similar profile for all complexes, despite the small differences observed between the complexes. According to Figure 10, the components ΔE_1^{orb} and ΔE_2^{orb} are related to the ligand-metal donation, while the components ΔE_3^{orb}, ΔE_4^{orb}, and ΔE_5^{orb} with the back donation. In fact, the sum of these contributions ($\Delta E_1^{orb} + \Delta E_2^{orb}$) and ($\Delta E_3^{orb} + \Delta E_4^{orb} + \Delta E_5^{orb}$) can be used to estimate the total ligand-metal donation and metal-ligand backdonation, respectively. The results indicate that the ligand-metal donation is the dominant term of the M-(YHE)cyclophane (Y = N, P; E = C, Si, Ge) complexes. The donation is slightly larger in silylenes derivative (**4**, **5**, **6**) than in carbenes (**1**, **2**, **3**) or germylenes (**7**, **8**, **9**). These findings are in agreement with the electron density laplacian plots of complexes **1**-**9**, which show that the charge concentration areas (red lines) distorted toward to the ruthenium atom are larger in silylenes (**4**, **5**, and **6**) than in carbenes (**1**, **2**, and **3**) or germylenes (**7**, **8**, and **9**) (supporting information Figure S6). For the complexe containing PHC (**3**), the ligand-metal donation is more stabilizing than in **1** or **2**. However this trend is not observed for silylenes or germylenes. The influence of back-donation was found to be a bit stronger in carbenes than in silylenes or germylenes.

4 Conclusions

The binding interactions between the $Ru(II)Cl^+$ and *ortho*-xylylene-linked-*bis*(YHE)cyclophane ligands (Y = N, P; E = C, Si, Ge) (**1**-**9**) yield very strong bonds. The observed trend of the metal-ligand bond strengths is that Ru(II)-NHC bonds are stronger than Ru(II)-NHSi and Ru(II)-NHGe. The strongest bond is predicted for the complex containing *ortho*-xylylene-linked-*bis*(PHC)cyclophane ligand (**3**), (ΔE^{int} = -345.0 kcal.mol^{-1}), which is due to the increase of the orbital ΔE_{tot}^{orb} and the decrease of the electrostatic contributions. In general, ligand-metal donation is the dominant term of the Ru-(YHE)cyclophane (Y = N, P; E = C, Si, Ge) complexes interactions. The role of metal-ligand back-donation for Ru-(YHE)cyclophane bonding is smaller than the ligand-metal donation, but it depends on the nature of the donor atom and is slightly stronger in carbenes than in silylenes or germylenes. The results reveal that the ruthenium(II)-[(η^1-NHC)$_2$: (η^6-arene)] are more covalently than electrostatically bonded and that the degree of covalence is larger in complexes containing PHCs than in complexes with NHCs or Enders' carbenes. They also reveal that the covalent character in ruthenium(II)-[(η^1-NHGe)$_2$: (η^6-arene)] and ruthenium(II)-[(η^1-NHSi)$_2$: (η^6-arene)] bonds is larger

than in ruthenium(II)-[(η^1-NHC)$_2$: (η^6-arene)].

5 Acknowledgements

The authors thank the National Council for Scientific and Technological Development (CNPq) for the financial support (grant 470985/2011-9) and the excellent service of the Hochschulrechenzentrum of the Philipps-Universitt Marburg. G.F.C. thanks the Coordination for the Improvement of Higher Level -or Education- Personnel (Capes) for the postdoctoral research scholarship (grant 3181-13-8). D.M.A. thanks the Deutscher Akademischer Austauschdienst for a postdoctoral scholarship.

References

1 G. P. Moss, P. A. S. Smith and D. Tavernier, *Pure and Appl. Chem.*, 1995, **67**, 1307–1375.
2 V. Boekelheide, *Acc. Chem. Res.*, 1980, **13**, 65–70.
3 R. Gleiter and D. Kratz, *Acc. Chem. Res.*, 1993, **26**, 311–318.
4 G. J. Bodwell and T. Satou, *Angew. Chem. Int. Ed.*, 2002, **41**, 4003–4006.
5 *Modern Cyclophane Chemistry*, ed. e. R. Gleiter and e. H. Hopf, Wiley-VCH Verlag GmbH & Co. KGaA, 2005, pp. i–xx.
6 J. Schulz and F. Vgtle, *Cyclophanes*, Springer Berlin Heidelberg, 1994, pp. 41–86.
7 P. J. Dyson, B. F. G. Johnson and C. M. Martin, *Coord. Chem. Rev.*, 1998, **175**, 59–89.
8 D. Braga, F. Grepioni and G. R. Desiraju, *Chem. Rev.*, 1998, **98**, 1375–1406.
9 M. Munakata, L. P. Wu and G. L. Ning, *Coord. Chem. Rev.*, 2000, **198**, 171–203.
10 M. Oh, G. B. Carpenter and D. A. Sweigart, *Acc. Chem. Res.*, 2004, **37**, 1–11.
11 M. Oh, J. A. Reingold, G. B. Carpenter and D. A. Sweigart, *Coord. Chem. Rev.*, 2004, **248**, 561–569.
12 A. K. Kakkar, *Chem. Rev.*, 2002, **102**, 3579–3588.
13 R. H. Fish and G. Jaouen, *Organometallics*, 2003, **22**, 2166–2177.
14 M. Munakata, S. Q. Liu, H. Konaka, T. Kuroda-Sowa, Y. Suenaga, M. Maekawa, H. Nakagawa and Y. Yamazaki, *Inorg. Chem.*, 2004, **43**, 633–641.
15 R. Rathore, V. J. Chebny and S. H. Abdelwahed, *J. Am. Chem. Soc.*, 2005, **127**, 8012–8013.
16 D. H. Camacho and Z. Guan, *Macromolecules*, 2005, **38**, 2544–2546.
17 D. H. Camacho, E. V. Salo, J. W. Ziller and Z. Guan, *Angew. Chem. Int. Ed.*, 2004, **43**, 1821–1825.
18 H. Hopf, *Angew. Chem. Int. Ed.*, 2008, **47**, 9808–9812.
19 C. J. Jones, *Chem. Soc. Rev.*, 1998, **27**, 289–300.
20 R. Hoffmann, *Acc. Chem. Res.*, 1971, **4**, 1–9.
21 M. N. Paddon-Row, *Acc. Chem. Res.*, 1982, **15**, 245–251.
22 G. F. Caramori and S. E. Galembeck, *J. Phys. Chem. A*, 2008, **112**, 11784–11800.
23 G. F. Caramori and S. E. Galembeck, *J. Phys. Chem. A*, 2007, **111**, 1705–1712.
24 G. F. Caramori, S. E. Galembeck and K. K. Laali, *J. Org. Chem.*, 2005, **70**, 3242–3250.
25 E. Heilbronner and Z.-z. Yang, *Cyclophanes II*, Springer Berlin Heidelberg, 1983, pp. 1–55.
26 F. Gerson, *Cyclophanes II*, Springer Berlin Heidelberg, 1983, pp. 57–105.
27 V. Boekelheide, *Acc. Chem. Res.*, 1980, **13**, 65–70.
28 T. Satou, K. Takehara, M. Hirakida, Y. Sakamoto, H. Takemura, H. Miura, M. Tomonou and T. Shinmyozu, *J. Organomet. Chem.*, 1999, **577**, 58–68.
29 R. J. Lavallee and C. Kutal, *J. Organomet. Chem.*, 1998, **562**, 97–104.
30 E. D. Laganis, R. H. Voegeli, R. T. Swann, R. G. Finke, H. Hopf and V. Boekelheide, *Organometallics*, 1982, **1**, 1415–1420.
31 C. Creutz and H. Taube, *J. Am. Chem. Soc.*, 1969, **91**, 3988–3989.
32 E. Laganis, R. Finke and V. Boekelheide, *Tetrahedron Lett.*, 1980, **21**, 4405–4408.
33 R. Finke, R. Voegeli, E. Laganis and V. Boekelheide, *Organometallics*, 1983, **2**, 347–350.
34 W. Rohrbach and V. Boekelheide, *J. Org. Chem.*, 1983, **48**, 3673–3678.
35 R. Swann and V. Boekelheide, *Tetrahedron Lett.*, 1984, **25**, 899–900.
36 V. Boekelheide, *Pure Appl. Chem.*, 1986, **58**, 1–6.
37 R. Swann, A. Hanson and V. Boekelheide, *J. Am. Chem. Soc.*, 1986, **108**, 3324–3334.
38 R. Voegeli, H. Kang, R. Finke and V. Boekelheide, *J. Am. Chem. Soc.*, 1986, **108**, 7010–7016.
39 M. V. Baker, M. J. Bosnich, C. C. Williams, B. W. Skelton and A. H. White, *Aust. J. Chem.*, 1999, **52**, 823–826.
40 M. Baker and D. Brown, *Mini-Reviews in Organic Chemistry*, 2006, **3**, 333–354.
41 M. V. Baker, B. W. Skelton, A. H. White and C. C. Williams, *J. Chem. Soc. Dalton Trans.*, 2001, 111–120.
42 M. V. Baker, M. J. Bosnich, D. H. Brown, L. T. Byrne, V. J. Hesler, B. W. Skelton, A. H. White and C. C. Williams, *J. Org. Chem.*, 2004, **69**, 7640–7652.
43 I. Bitter, Z. Torok, V. Csokai, A. Grun, B. Balazs, G. Toth, G. M. Keseru, Z. Kovari and M. Czugler, *Eur. J. Org. Chem.*, 2001, 2861–2868.
44 J. Yoon, S. K. Kim, N. J. Singh and K. S. Kim, *Chem. Soc. Rev.*, 2006, **35**, 355–360.
45 P. A. Gale, S. E. Garcia-Garrido and J. Garric, *Chem. Soc. Rev.*, 2008, 151–190.
46 C. Caltagirone and P. A. Gale, *Chem. Soc. Rev.*, 2009, **38**, 520–563.
47 J. C. Garrison, R. S. Simons, J. M. Talley, C. Wesdemiotis, C. A. Tessier and W. J. Youngs, *Organometallics*, 2001, **20**, 1276–1278.
48 J. C. Garrison, R. S. Simons, C. A. Tessier and W. J. Youngs, *J. Organomet. Chem.*, 2003, **673**, 1–4.
49 M. V. Baker, S. K. Brayshaw, B. W. Skelton, A. H. White and C. C. Williams, *J. Organomet. Chem.*, 2005, **690**, 2312–2322.
50 P. J. Barnard, L. E. Wedlock, M. V. Baker, S. J. Berners-Price, D. A. Joyce, B. W. Skelton and J. H. Steer, *Angew. Chem. Int. Ed.*, 2006, **45**, 5966–5970.
51 O. Kaufhold, A. Stasch, T. Pape, A. Hepp, P. G. Edwards, P. D. Newman and F. E. Hahn, *J. Am. Chem. Soc.*, 2009, 306–317.
52 M. V. Baker, D. H. Brown, P. V. Simpson, B. W. Skelton, A. H. White and C. C. Williams, *J. Oraganomet. Chem.*, 2006, **691**, 5845–5855.
53 F. E. Hahn, V. Langenhahn, T. Lgger, T. Pape and D. Le Van, *Angew. Chem. Int. Ed.*, 2005, **44**, 3759–3763.
54 F. E. Hahn, C. Radloff, T. Pape and A. Hepp, *Chem. A Eur. J.*, 2008, **14**, 10900–10904.
55 M. V. Baker, D. H. Brown, V. J. Hesler, B. W. Skelton and A. H. White, *Organometallics*, 2007, **26**, 250–252.
56 M. V. Baker, D. H. Brown, R. A. Haque, B. W. Skelton and A. H. White, *Dalton Trans.*, 2010, **39**, 70–72.
57 I. Özdemir, S. Demir, N. Gürbüz, B. Çetinkaya, L. Toupet, C. Bruneau and P. H. Dixneuf, *Eur. J. Inorg. Chem.*, 2009, **2009**, 1942–1949.
58 I. Özdemir, S. Demir, B. Çetinkaya, L. Toupet, R. Castarlenas, C. Fischmeister and P. H. Dixneuf, *Eur. J. Inorg. Chem.*, 2007, 2862–2869.

This journal is © The Royal Society of Chemistry [year]

59 B. Çetinkaya, S. Demir, I. Özdemir, L. Toupet, D. Sémeril, C. Bruneau and P. H. Dixneuf, *Chem. A Eur. J.*, 2003, **9**, 2323–2330.
60 S. H. Hong, A. Chlenov, M. W. Day and R. H. Grubbs, *Angew. Chem. Int. Ed.*, 2007, **46**, 5148–5151.
61 D. Enders, K. Breuer, G. Raabe, J. Runsink, J. H. Teles, J.-P. Melder, K. Ebel and S. Brode, *Angew. Chem. Int. Ed.*, 1995, **34**, 1021–1023.
62 A. Fekete and L. Nyulszi, *J. Organomet. Chem.*, 2002, **643–644**, 278–284.
63 W. W. Schoeller and D. Eisner, *Inorg. Chem.*, 2004, **43**, 2585–2589.
64 D. Martin, A. Baceiredo, H. Gornitzka, W. W. Schoeller and G. Bertrand, *Angew. Chem. Int. Ed.*, 2005, **117**, 1728–1731.
65 H. Jacobsen, *J. Organomet. Chem.*, 2005, **690**, 6068–6078.
66 J. D. Masuda, D. Martin, C. Lyon-Saunier, A. Baceiredo, H. Gornitzka, B. Donnadieu and G. Bertrand, *Chem. Asian J.*, 2007, **2**, 178–187.
67 M. Rullich, R. Tonner and G. Frenking, *New J. Chem.*, 2010, **34**, 1760–1773.
68 J. Kapp, C. Schade, A. M. El-Nahasa and P. von Ragu Schleyer, *Angew. Chem. Int. Ed.*, 1996, **35**, 2236–2238.
69 M. Denk, R. Lennon, R. Hayashi, R. West, A. V. Belyakov, H. P. Verne, A. Haaland, M. Wagner and N. Metzler, *J. Am. Chem. Soc.*, 1994, **116**, 2691–2692.
70 M. Haaf, A. Schmiedl, T. A. Schmedake, D. R. Powell, A. J. Millevolte, M. Denk and R. West, *J. Am. Chem. Soc.*, 1998, **120**, 12714–12719.
71 M. Driess, S. Yao, M. Brym, C. van Wllen and D. Lentz, *J. Am. Chem. Soc.*, 2006, **128**, 9628–9629.
72 C.-W. So, H. W. Roesky, J. Magull and R. B. Oswald, *Angew. Chem.*, 2006, **118**, 4052–4054.
73 S. S. Sen, H. W. Roesky, D. Stern, J. Henn and D. Stalke, *J. Am. Chem. Soc.*, 2010, **132**, 1123–1126.
74 B. Blom, M. Stoelzel and M. Driess, *Chem. A Eur. J.*, 2013, **19**, 40–62.
75 A. Meller and C.-P. Gräbe, *Chem. Ber.*, 1985, **118**, 2020–2029.
76 C. Heinemann, W. A. Herrmann and W. Thiel, *J. Organomet. Chem.*, 1994, **475**, 73–84.
77 O. Kühl, *Coord. Chem. Rev.*, 2004, **248**, 411–427.
78 H. Jacobsen, A. Correa, A. Poater, C. Costabile and L. Cavallo, *Coord. Chem. Rev.*, 2009, **253**, 687–703.
79 O. Khl, K. Lifson and W. Langel, *Eur. J. Org. Chem.*, 2006, 2336–2343.
80 T. J. Hadlington, M. Hermann, J. Li, G. Frenking and C. Jones, *Angew. Chem.*, 2013, **125**, 10389–10393.
81 P. Hohenberg and W. Kohn, *Phys. Rev.*, 1964, **136**, B864–B871.
82 W. Kohn and L. J. Sham, *Phys. Rev.*, 1965, **140**, A1133–A1138.
83 A. D. Becke, *Phys. Rev. A*, 1988, **38**, 3098–3100.
84 J. P. Perdew, *Phys. Rev. B*, 1986, **33**, 8822–8824.
85 S. Grimme, *J. Comput. Chem.*, 2006, **27**, 1787–1799.
86 S. Grimme, S. Ehrlich and L. Goerigk, *J. Comput. Chem.*, 2011, **32**, 1456–1465.
87 S. Grimme, *WIREs Comput. Molec. Sci.*, 2011, **1**, 211–228.
88 F. Weigend and R. Ahlrichs, *Phys. Chem. Chem. Phys.*, 2005, **7**, 3297–3305.
89 F. Weigend, *Phys. Chem. Chem. Phys.*, 2006, **8**, 1057–1065.
90 E. v. Lenthe, E. J. Baerends and J. G. Snijders, *J. Chem. Phys.*, 1993, **99**, 4597–4610.
91 M. Filatov, *Chem. Phys. Chem.*, 2002, **365**, 222–231.
92 C. v. Wüllen, *J. Chem. Phys.*, 1998, **109**, 392–399.
93 F. Neese, *WIREs Comput. Mol. Sci.*, 2012, **2**, 73–78.
94 M. P. Mitoraj, A. Michalak and T. Ziegler, *J. Chem. Theory Comput.*, 2009, **5**, 962–975.
95 J. P. Foster and F. Weinhold, *J. Am. Chem. Soc.*, 1980, **102**, 7211–7218.
96 A. E. Reed and F. Weinhold, *J. Chem. Phys.*, 1983, **78**, 4066–4073.
97 A. E. Reed, L. A. Curtiss and F. Weinhold, *Chem. Rev.*, 1988, **88**, 899–926.
98 E. D. Glendening, C. R. Landis and F. Weinhold, *WIREs Comput. Mol. Sci.*, 2012, **2**, 1–42.
99 C. F. Matta and R. J. Boyd, *The Quantum Theory of Atoms in Molecules*, Wiley-VCH Verlag GmbH & Co. KGaA, 2007, pp. 1–34.
100 R. F. W. Bader, *Atoms in molecules: a quantum theory*, Clarendon Press, Oxford; New York, 1990.
101 E. Van Lenthe and E. J. Baerends, *J. Comput. Chem.*, 2003, **24**, 1142–1156.
102 G. te Velde, F. M. Bickelhaupt, E. J. Baerends, C. Fonseca Guerra, S. J. A. van Gisbergen, J. G. Snijders and T. Ziegler, *J. Comput. Chem.*, 2001, **22**, 931–967.
103 C. F. Guerra, J. G. Snijders, G. t. Velde and E. J. Baerends, *Theor. Chem. Acc.*, 1998, **99**, 391–403.
104 T. Ziegler and A. Rauk, *Inorg. Chem.*, 1979, **18**, 1755–1759.
105 T. Ziegler and A. Rauk, *Theoret. Chim. Acta*, 1977, **46**, 1–10.
106 M. Mitoraj and A. Michalak, *J. Mol. Model.*, 2007, **13**, 347–355.
107 A. Michalak, M. Mitoraj and T. Ziegler, *J. Phys. Chem. A*, 2008, **112**, 1933–1939.
108 M. Mitoraj and A. Michalak, *Organometallics*, 2007, **26**, 6576–6580.
109 M. Mitoraj and A. Michalak, *J. Mol. Model.*, 2008, **14**, 681–687.
110 M. P. Mitoraj, H. Zhu, A. Michalak and T. Ziegler, *Int. J. Quantum Chem.*, 2009, **109**, 3379–3386.
111 M. P. Mitoraj and A. Michalak, *Inorg. Chem.*, 2010, **49**, 578–582.
112 I. Cukrowski, K. K. Govender, M. P. Mitoraj and M. Srebro, *J. Phys. Chem. A*, 2011, **115**, 12746–12757.
113 M. P. Mitoraj, *J. Phys. Chem. A*, 2011, **115**, 14708–14716.
114 M. von Hopffgarten and G. Frenking, *J. Phys. Chem. A*, 2011, **115**, 12758–12768.
115 F. Neese, *J. Phys. Chem. Sol.*, 2004, **65**, 781–785.
116 D. Herebian, E. Bothe, F. Neese, T. Weyhermller and K. Wieghardt, *J. Am. Chem. Soc.*, 2003, **125**, 9116–9128.
117 E. Miliordos, K. Ruedenberg and S. S. Xantheas, *Angew. Chem. Int. Ed.*, 2013, **52**, 5736–5739.
118 H.-J. Werner, P. J. Knowles, G. Knizia, F. R. Manby and M. Schütz, *WIREs Comput Mol Sci*, 2012, **2**, 242–253.
119 H.-J. Werner, P. J. Knowles, G. Knizia, F. R. Manby, M. Schütz *et al.*, *MOLPRO, version 2012.1, a package of ab initio programs*, 2012.
120 C. Boehme and G. Frenking, *Organometallics*, 1998, **17**, 5801–5809.
121 G. Frenking, M. Sol and S. F. Vyboishchikov, *J. Organomet. Chem.*, 2005, **690**, 6178–6204.
122 N. S. Antonova, J. J. Carb and J. M. Poblet, *Organometallics*, 2009, **28**, 4283–4287.
123 N. S. Antonova, J. J. Carb and J. M. Poblet, *Dalton Trans.*, 2011, **40**, 2975–2982.
124 G. F. Caramori, L. C. Garcia, D. M. Andrada and G. Frenking, *Organometallics*, 2014, **33**, 2301–2312.

This journal is © The Royal Society of Chemistry [year]

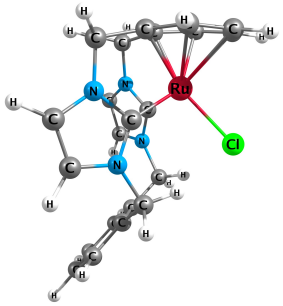

The metal-ligand bonds in ruthenium(II) complexes of N-heterocyclic carbenes derived from Imidazolium-linked cyclophanes with a remarkable covalent character.